Proc. Natl. Acad. Sci. USA
Vol. 94, pp. 4554–4559, April 1997
Genetics

Defective "pacemaker" current (I_h) in a zebrafish mutant with a slow heart rate

KEITH BAKER*†, KERRI S. WARREN‡§, GARY YELLEN*, AND MARK C. FISHMAN‡¶

Departments of *Neurobiology and †Anesthesia and the ‡Cardiovascular Research Center, Harvard Medical School and Massachusetts General Hospital, Boston, MA 02114

Communicated by Alexander Leaf, Massachusetts General Hospital, Charlestown, MA, February 21, 1997 (received for review November 8, 1996)

ABSTRACT **At a cellular level, cardiac pacemaking, which sets the rate and rhythm of the heartbeat, is produced by the slow membrane depolarization that occurs between action potentials. Several ionic currents could account for this pacemaker potential, but their relative prominence is controversial, and it is not known which ones actually play a pacemaking role *in vivo*. To correlate currents in individual heart cells with the rhythmic properties of the intact heart, we have examined *slow mo (smo)*, a recessive mutation we discovered in the zebrafish *Danio rerio*. This mutation causes a reduced heart rate in the embryo, a property we can quantitate because the embryo is transparent. We developed methods for culture of cardiocytes from zebrafish embryos and found that, even in culture, cells from *smo* continue to beat relatively slowly. By patch-clamp analysis, we discovered that a large repertoire of cardiac currents noted in other species are present in these cultured cells, including sodium, T-type, and L-type calcium and several potassium currents, all of which appear normal in the mutant. The only abnormality appears to be in a hyperpolarization-activated inward current with the properties of I_h, a current described previously in the nervous system, pacemaker, and other cardiac tissue. *smo* cardiomyocytes have a reduction in I_h that appears to result from severe diminution of one kinetic component of the I_h current. This provides strong evidence that I_h is an important contributor to the pacemaking behavior of the intact heart.**

During the relaxation phase of the heart (diastole), cells of the normal pacemaker region exhibit a slow depolarization that brings the membrane potential up to the threshold for the next action potential and hence has been termed the "pacemaker potential." Several currents contribute to the pacemaker potential, but there is debate about their relative importance for pacemaking (1–3). One proposal is that the pacemaker potential is due principally to the decay of the potassium-delayed rectifier current (I_{Kr}) in combination with a time-independent inward background current (possibly supplied by the Na^+–Ca^{2+} exchanger) (4). Another view is that the slow depolarization is due to the I_h current, a nonselective Na^+/K^+ conductance activated upon hyperpolarization in a time-dependent fashion (5, 6). This current is also referred to as I_f (7), or as the pacemaker current, because it was first described in cells of the pacemaker region (8, 9). In fact, I_h is present in cells throughout the Purkinje system (10–12) and even in ventricular myocytes, where it is activated at more hyperpolarized voltages than in the sino-atrial node (13, 14). I_h also is found in some neurons. For instance, in the thalamus, it helps to generate sleep-regulated oscillatory rhythms (15).

To understand the roles of single genes in the development of organ function, we undertook a large-scale screen for mutations that affect the heart in the embryo of the zebrafish *Danio rerio* (16). The embryos of this vertebrate are transparent, so cardiac function can be analyzed in real time. The chamber design and function of the 2-day postfertilization embryonic fish heart is quite similar to that of the 3-week gestation human embryo heart. Unlike the human, the fish embryo does not depend for survival upon its circulation at the early stages because diffusion suffices (16–18). Therefore, mutants can survive without any functioning heart beat for days and can be studied specifically with regard to cardiac effects without complications due to nutritional deficiency or secondary deterioration. As part of our screen, we discovered 57 recessive mutations that affect the heart or vessels (16).

Of these zebrafish mutations, one, *slow mo*, affects the heart rate. From the onset of regular contractions, the mutant heart rate is slower than wild type, a condition termed "bradycardia." This appears to be due to the properties of individual heart cells because they beat slowly compared with wild type even after dissociation into cell culture. Of the several potential pacemaking currents, only I_h is perturbed in the mutants. There is a severe reduction in the fast kinetic component whereas a slow component of I_h remains intact. Thus, selective diminution of one component of I_h, as assayed in individual cells, appears to cause bradycardia but otherwise does not perturb cardiac development.

MATERIALS AND METHODS

Cardiomyocyte Culture. Care and breeding of zebrafish (*D. rerio*) was as described (19). Developmental staging was carried out using standard morphological features (20) of fish raised at 28.5°C. The zebrafish embryo is transparent, so phenotypic characterization and all heart rate data were obtained by direct visual inspection under a dissecting microscope. Throughout this paper, "*smo*" refers to fish or cells that are homozygous for the *smo* mutation. The hearts from tricaine-anesthetized day 3 embryos were removed and placed in L15 media, rinsed in Hanks' balanced salt solution, and incubated in collagenase type II (250 units/ml) and protease type XIV (1.0 unit/ml) with trituration to isolate the cardiomyocytes. Cells were plated on polylysine-coated coverslips and incubated in L15 supplemented with 10% fetal bovine serum and 1% penicillin/streptomycin at 28.5°C. For dissociated beat rate analysis, cell clusters were cultured for 1–4 h. For patch-clamp recording, all cells were used 18–36 h after plating to allow for single cell attachment onto coverslips. Only healthy cultures with beating cells were used for analysis.

Patch-Clamp Recording. Standard whole cell recording techniques (21) were applied to single cells. All data were

The publication costs of this article were defrayed in part by page charge payment. This article must therefore be hereby marked "*advertisement*" in accordance with 18 U.S.C. §1734 solely to indicate this fact.

0027-8424/97/944554-6$2.00/0
PNAS is available online at **http://www.pnas.org**.

¶To whom reprint requests should be addressed at: Cardiovascular Research Center, Massachusetts General Hospital-East, 149 13th Street, 4th Floor, Charlestown, MA 02129. email: fishman@cvrc.mgh.harvard.edu.
§K.B. and K.S.W. contributed equally to this paper.

acquired and analyzed blind to the genotype. For I_h and I_{Kr}, bath solution contained (in mM): NaCl 135, KCl 20, $MgCl_2$ 1, $CaCl_2$ 2, Hepes 10, and glucose 10 (pH 7.4 with NaOH). Pipette solution contained (in mM): KF 70, KCl 70, $MgCl_2$ 0.5, Hepes 10, and EGTA 10 (pH 7.4 with NaOH). For $I_{Ca,T}$, bath solution contained (in mM): $CaCl_2$ 15, CsCl 5, Hepes 10, glucose 10, and *N*-methyl-D-glucamine 125 (pH 7.4 with HCl). Pipette solution contained (in mM): tetraethylammonium-chloride 140, $MgCl_2$ 0.5, Hepes 1, and EGTA 1 (pH 7.4 with CsOH). Pipettes were coated with Sylgard (Dow Corning, Midland, MI) and fire polished to resistances of 2–5 MΩ. Data acquisition and analysis were carried out using pClamp6 software (Axon Instruments, Foster City, CA). All recordings were at room temperature (21–23°C). For comparison of I_h and I_{Kr} from the same cell, the amplitude of the I_h current was determined from the amplitude of the Boltzmann fit, and the amplitude of the I_{Kr} current was determined in an analogous fashion. The leak current and nonlinear open channel properties were minimized for both the I_h and I_{Kr} records by taking all of the current amplitudes at a constant voltage.

The kinetics of activation for I_h were determined at −130 mV. Data traces were filtered at 1 kHz and fitted with either a single or double exponential curve. All traces were initially fit with a single exponential. The need for a second component was determined by a trial fit with two components. If the fitting algorithm converged and gave a nontrivial second component (i.e., time constant and amplitude > 0), then two components were assumed. The fitting and number of components was determined blind to the genotype. In most cases, the number of components was easily confirmed by visual inspection.

RESULTS

***slow mo* Mutants Have a Reduced Heart Rate.** The *smo* mutation is evident as a slow heartbeat in 25% of embryos from a *smo*± × *smo*± cross, a recessive inheritance pattern that has been evident over seven generations. The heart and the embryo appear otherwise normal, and there is no evidence for diminished viability of *smo*−/− embryos compared with wild type at 28.5°C. Homozygotes have been raised to adulthood and can breed successfully. No other alleles of this mutation were isolated among the combined 6647 mutations generated in the two recent, large-scale screens (16, 22).

In the wild-type zebrafish embryo, the single heart tube is silent at the time it is generated by fusion of the bilateral tubes. Isolated twitches begin diffusely in the myocardium at 21 h postfertilization (hpf), followed by irregular peristaltic motions, which flow in a wave from the venous to arterial end. By 24 h postfertilization, there are regular peristaltic contractions, which establish blood flow through the circulation, and by 32 h postfertilization, there are sequential contractions of the atrium followed by the ventricle.

smo mutants have a reduced heart rate from the onset of regular contractions in the heart tube. The wild-type heart rate increases in the first days postfertilization, as it does in other species (17), and even the early embryo responds to warming with an increased rate and to cooling with a decreased rate (Fig. 1*A*). The heart rate of *smo* mutants is significantly slower at all stages of development and at all temperatures (Fig. 1*B*), and the temperature response is abnormal (warming diminishes the rate).

The intrinsic heart rate in *smo* embryos is slow before innervation, suggesting that the *smo* defect is not directly neural in nature. In fact, when embryonic hearts are explanted into culture, the difference between wild type and *smo* beat rates is still apparent. Day 3 *smo* extracted hearts beat at 46.9 ± 3.7 beats per minute (mean ± SD; $n = 48$) whereas wild-type hearts beat at 78.7 ± 6.2 beats per minute (mean ± SD; $n = 50$; significant, $P < 0.0005$). To rule out selective failure of specialized pacemaker or conduction tissue within the intact

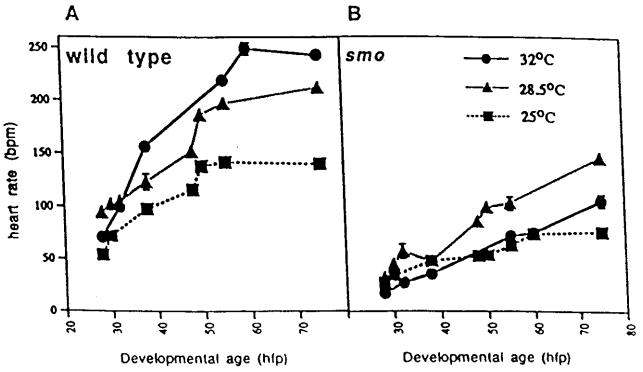

FIG. 1. The heart rate in *smo* homozygotes is slow throughout development and at different temperatures. Heart rates were counted upon visual inspection of unanesthetized embryos developing at room temperature (25°C), our standard aquaculture temperature (28.5°C), or at an elevated temperature (32°C). At least 40 animals were examined for each time point at each temperature. The heart rates of both the wild type siblings (*A*) and *smo* mutants (*B*) rose with developmental stage at all temperatures examined. *Smo* heart rates were consistently lower than wild type. Additionally, as shown in *A*, wild type hearts were very responsive to shifts in temperature. The mutant hearts (*B*), however, had an abnormal decrease in heart rate when raised at 32°C. hpf, hours postfertilization.

smo heart, we dissociated hearts into small clusters of cells and found that *smo* cardiomyocyte clusters beat slower than wild type clusters [wild type 39.6 ± 11.8 beats per minute (mean ± SD; $n = 30$); *smo* 20.8 ± 4.6 beats per minute (mean ± SD; $n = 30$; significant, $P < 0.0005$)]. Because the *smo* phenotype present in the mutant fish persists even when *smo* hearts are dispersed in culture, we reasoned that the defect may be present in single cells. We therefore developed methods for isolated cardiomyocyte culture and electrophysiological analysis of individual cells from wild type or *smo* hearts.

Embryonic Cardiocytes Have a Hyperpolarization-Activated Inward Current. We examined channel activity in individual dissociated cardiomyocytes by voltage clamp. Embryonic zebrafish cardiocytes have, as described in embryonic hearts of other species, voltage-gated sodium currents (I_{Na}), L-type calcium currents ($I_{Ca,L}$), and T-type calcium currents ($I_{Ca,T}$), as well as potassium currents with the properties of an ultrarapid delayed rectifier ($I_{K,ur}$), transient outward (I_A), and a rapid delayed rectifier with inward rectification (I_{Kr}) (unpublished work). These did not appear different between wild-type and *smo* mutant fish (data not shown).

We also identified a hyperpolarization-activated current with properties that correspond to I_h noted previously (11). As shown in Fig. 2, this current meets the criteria for I_h because it is an inward current, carried by both Na^+ and K^+. In the cardiocytes, it is evident as a slowly activating current that appears when the membrane voltage is stepped from a holding voltage of −40 mV to more negative voltages (Fig. 2*A*). This inward current is due to an increase in conductance, measured by the instantaneous change in current upon stepping to a different voltage after activation (Fig. 2*B*). The conductance continues to increase with more negative activating voltages, reaching a half-maximal value by ≈−95 mV. The conductance has a reversal potential of ≈−14 mV, compared with the potassium equilibrium potential of −49 mV (Fig. 2*B*, bottom). This is compatible with the known properties of I_h in other systems (11). The current is blocked completely by 2 mM extracellular Cs^+, as is I_h elsewhere (23, 24) (Fig. 2*C*).

***smo* Mutants Have Diminished I_h.** For quantitation, we focused on currents potentially involved in diastolic depolarization, including $I_{Ca,T}$, the delayed rectifier, I_{Kr}, and I_h. We found a substantial and specific reduction of I_h in cardiocytes of *smo* mutants compared with wild type over the entire

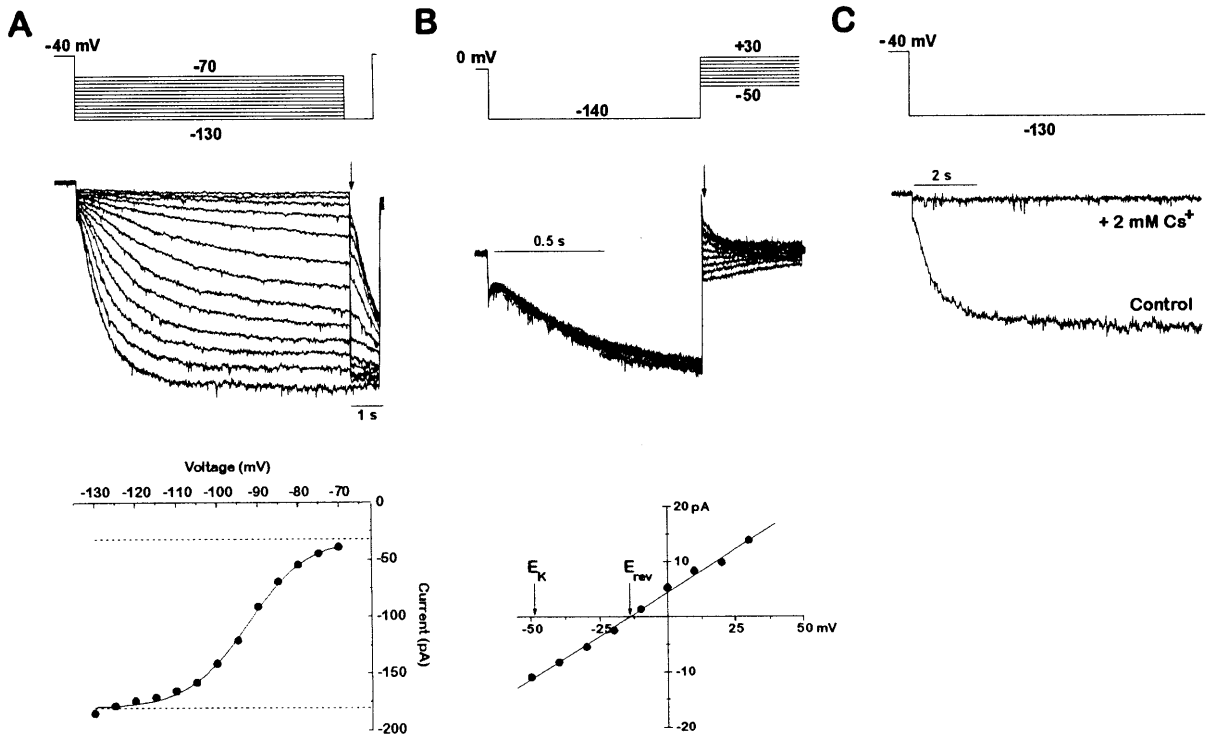

FIG. 2. A hyperpolarization-activated I_h current is present in zebrafish cardiac myocytes. (*A*) Activation of I_h current by hyperpolarization. An individual dissociated cardiomyocyte was voltage-clamped from a holding potential of −40 mV to various hyperpolarizing voltages (−70 to −130 mV in 10-mV increments) once every 15 s. Each hyperpolarization was followed by a step to −130 mV to determine the current at a constant voltage. The current amplitude immediately after the voltage step to −130 mV was then plotted as a function of the activation voltage. The data were fitted with a Boltzmann function. The amplitude of the I_h current was given by the net amplitude of the Boltzmann function. The leak current was determined by the baseline of the fit and was not part of the I_h determination. Current traces were filtered at 1 kHz. (*B*) Tail current analysis of the I_h reversal potential. After I_h was activated for 1 s by a step from 0 mV to −130 mV, another step was applied to a new voltage (from −50 to +30 mV in 10-mV increments). The tail current amplitude immediately after the voltage clamp settled is plotted as a function of the tail current voltage. The tail currents reversed at −14 mV, as determined by the line fitted to the data points. A perfectly potassium-selective channel would have a reversal potential of −49 mV in the solutions used. The dihydropyridine niguldipine (1 μM) was included to block the calcium currents present in these cells. If the cell was held at 0 mV and not hyperpolarized to activate the I_h current, no tail currents were observed (data not shown). Current traces were filtered at 2 kHz. The voltage protocol was delivered once every 4 s. (*C*) Inhibition of I_h by cesium. I_h currents with and without 2 mM CsCl applied extracellularly, in response to a step from −40 mV to −130 mV. Current traces were filtered at 1 kHz.

voltage range of activation, from −65 to −130 mV. Fig. 3*A* shows representative recordings of I_h from a wild-type and a *smo* mutant cell, and 3*B* shows the quantitation for many cells measured at the test voltage of −130 mV. The amplitude of the I_h current at this test voltage is reduced by ≈85% in *smo*. As a control for conditions and cell viability, we assayed I_{Kr} in the same cells as I_h. We also measured $I_{Ca,T}$ because blockade of this current with Ni^{2+} is reported to slow the heart rate (1). There was no significant change in I_{Kr} or in $I_{Ca,T}$ (Fig. 3 *A* and *B*). Therefore, of the several currents potentially involved in pacemaking, only I_h appears to be affected by the mutation.

We noted that I_h in *smo* is diminished but not absent. There are several possibilities for this. One is that the mutation changes the properties of the I_h channel rather than eliminating its function. To examine this, we more closely studied its kinetic properties. In wild-type I_h, the kinetics of opening are well described by the sum of two exponentials, as shown in Fig. 4*A*. One component is larger and more rapidly activating and is referred to as "fast"; the other is smaller and more slowly activating and is referred to as "slow." The smaller I_h current in the *smo* mutant cells appears to consist mainly of the slow component (Fig. 4*A*). The fast component in *smo* cells is severely reduced, and in many cells it is undetectable (Fig. 4*B*). Although it is possible that *smo* causes interconversion of fast and slow components, this seems unlikely given that the slow component is unchanged in the mutant, both in its amplitude and kinetics. Rather, it appears that there may be two separate types of I_h channel corresponding to the currents with fast and slow kinetics and that the *smo* gene product is required, directly or indirectly, to generate a normal fast component.

DISCUSSION

We describe here a recessive mutation that causes a marked reduction in heart rate and is reflected at the cellular level by specific and selective perturbation of a single current, the hyperpolarization-activated cation current referred to as I_h. This provides strong genetic evidence that I_h helps control heart rate. The selective reduction of the fast kinetic component, with the maintenance of an intact slow component, suggests that there may be two channels normally involved in I_h and that this mutation severely affects the fast one.

There are two principal models for how pacemaking is achieved. These are not mutually exclusive, and, in fact, either could predominate in different pacemaker regions or at different stages of development. One places emphasis upon the delayed rectifier potassium current I_{Kr}, the current that underlies repolarization of the action potential. Pacemaking, by this model, is due to the decay of I_{Kr} combined with a time-independent depolarizing tendency due to background currents or to the Na^+–Ca^{2+} exchanger (4). We found that I_{Kr} and its decay at negative voltages are normal in the *smo* mutant (Fig. 3*A*).

The other model for pacemaking depends upon I_h. I_h is an inward Na^+ and K^+ current activated by hyperpolarization. Therefore, it is inactive until after the action potential, when

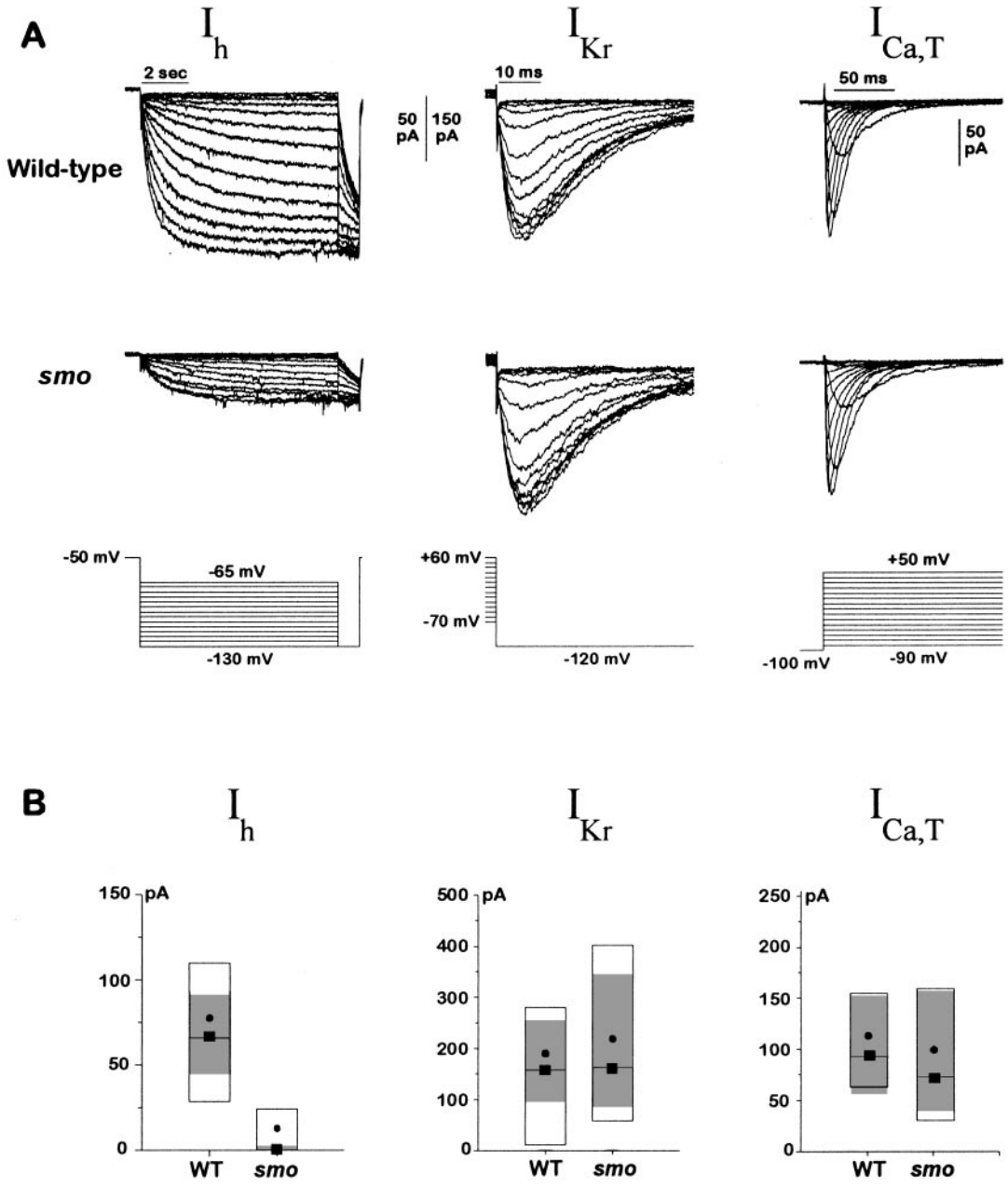

FIG. 3. I_h is reduced in *smo* cardiac myocytes. (*A*) Representative I_h, I_{Kr}, and $I_{Ca,T}$ currents from wild-type and *smo* cells. I_h was elicited from a holding voltage of −50 mV by steps to various voltages (−65 to −130 mV in 5-mV increments). A test voltage of −130 mV was applied at the end of each hyperpolarizing step. I_{Kr} was activated by a ≈1-s prepulse to various voltages (+60 to −70 mV in 10-mV increments); the inwardly rectifying current was then measured at a constant test voltage of −120 mV. $I_{Ca,T}$ was elicited from a holding potential of −100 mV to voltages ranging from −90 to +50 mV once every 2 s. Current traces were filtered at 1 kHz (I_h) or 5 kHz (I_{Kr} and $I_{Ca,T}$). (*B*) Amplitude of I_h, I_{Kr}, and $I_{Ca,T}$ currents from many wild-type and *smo* cells. The data are displayed as box plots. The box delimits the central 50% of the data values. The median is shown as a solid line tagged with a solid box, and the mean is shown as a solid circle. The 99% confidence interval for a robust median is shown by the gray shaded zone. The confidence interval is based on the biweight locator and estimate of scale (25). Boxplots of the I_h current amplitudes are shown for wild-type (n = 47) and *smo* (n = 48) cells. Boxplots of the I_{Kr} current amplitudes also are shown for wild-type (n = 31) and *smo* (n = 23) cells and for $I_{Ca,T}$, wild-type (n = 20), and *smo* (n = 20) cells. The size of whole cell I_h currents in *smo* cells was very small (average 12.0 pA), making it difficult to fit some of the data to a Boltzmann function. The amplitude comparison between wild-type and *smo* cells was thus repeated but with recording conditions that were chosen to enhance the amplitude of the I_h currents. The bath solution was as described in *Materials and Methods* except that KCl was increased to 140 mM, 2 mM $BaCl_2$ was added, and NaCl was omitted. The pipette solution was supplemented with 100 μM cAMP. The I_h current amplitude was indeed enhanced 2.5-fold by the changes in recording solutions, and the effects of the *smo* mutation on the I_h current were the same. For the I_h current, the confidence interval was 110–260 pA in wild-type cells (n = 19) compared with 5–44 pA in *smo* cells (n = 20). I_{Kr} current was again unchanged by the mutation: 99% confidence interval was 67–358 pA for wild-type (n = 20) and 109–261 pA for *smo* cells (n = 19). The reduction in I_h current in *smo* cells was not due to a difference in cell size between wild-type and *smo* because the cell capacitances were the same for the two genotypes; the 99% confidence interval on the robust median for wild-type (n = 34) was 2.3–3.2 pF and for *smo* (n = 28) was 2.4–3.1 pF. Data were obtained for both I_h and I_{Kr} from each cell whenever possible. The amplitude of the I_h current was determined as shown in Fig. 2*A* from the amplitude of the Boltzmann fit, and the amplitude of the I_{Kr} current was determined in an analogous fashion. The current amplitude for $I_{Ca,T}$ was determined at −20 mV after leak subtraction. The leak current and nonlinear open channel properties were minimized for both the I_h and I_{Kr} records by taking all of the current amplitudes at a constant voltage. For each value in the legend, we report a range of numbers giving the 99% confidence interval for the robust median. WT, wild-type.

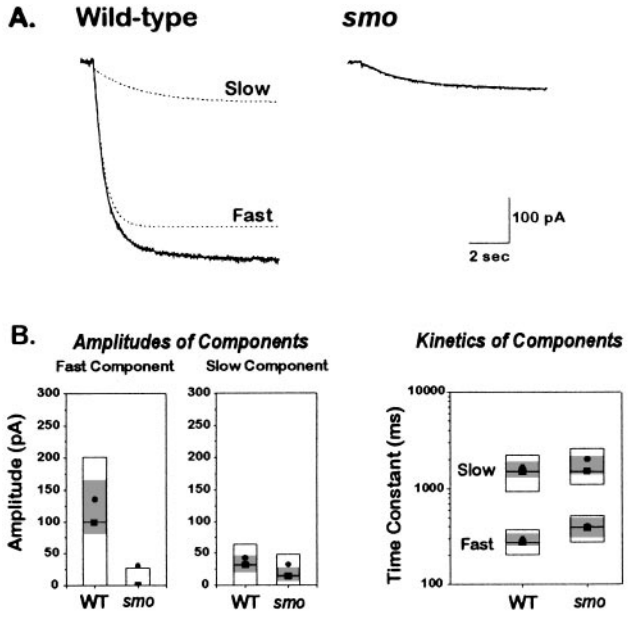

FIG. 4. The reduced I_h current in *smo* cells is due to the reduction of a fast component normally seen in wild type. (*A*) Representative I_h currents from a wild type and a *smo* cell in response to a step from −40 to −130 mV. I_h currents were recorded using the solutions noted in the Fig. 3 legend. The wild type current trace was fit with a sum of two exponentials; the individual exponential components are shown in the dashed lines, and their sum lies on top of the current trace. The *smo* current was well described by a single exponential. (*B*) Amplitude and kinetic analysis of wild type and *smo* I_h currents. Wild type I_h currents (from 68 cells) were fitted with two exponentials (Fast and Slow); the amplitude and time constant for each component are displayed separately. *smo* I_h currents (from 65 cells) were fitted with either one or two exponentials (Fast and Slow); the amplitude and time constant for each component are displayed separately. The amplitude of the fast component is markedly reduced in *smo* cells. The kinetics of both the fast and slow components are similar. The shaded area in each box shows the 99% confidence interval about the robust median. WT, wild type.

the membrane potential becomes sufficiently hyperpolarized. I_h activation at negative voltages should help depolarize the cell to threshold. I_h appears to be an important regulatory target of both cholinergic and adrenergic agents upon the heart (26–28). It is present in nodal cells but is not limited to them, and there is controversy about whether this current is really critical to pacemaking (12). One concern is that, in some cells, the activation range of I_h appears to be more negative than the range reached during diastole. An explanation for this discrepancy is that I_h may vary with assay conditions and so be underestimated. For example, the gating of I_h is sensitive to neurotransmitters and cAMP, and it may be difficult to mimic the normal extracellular or intracellular milieu in patch-clamp experiments on cultured cells. Therefore, it is particularly important that, using this mutant, we can correlate measurements of I_h activity in isolated cells with heart rate assays *in vivo* and can do so without reliance on pharmacological intervention.

The kinetics of activation of I_h in the wild-type cells are well accounted for by the sum of two exponentials. Only the fast component is affected in *smo*, and it is nearly eliminated. We suspect from this that I_h is due to activity of two distinct channels and that the *smo* mutation selectively affects one of them. There are alternative hypotheses. The data also could be explained by a single channel with kinetics altered by the mutation. This explanation seems unlikely because the slow component is apparently unchanged in the mutant. I_h has not been noted to have two components in prior studies of heart cells, but two kinetic components of I_h have been described in visual cortical projection neurons (29). In fact, some of these neurons have only the slow or fast forms, and some have both, lending credence to the notion that there are, potentially, two I_h channels.

Most cardiac cells have latent pacemaking properties, but in the intact heart, those at the sino-atrial node beat faster and thus override the other pacemakers. Consistent with this regional difference in pacemaking properties, I_h has been shown in other species to activate at less negative potentials in nodal cells than in ventricular cardiomyocytes (4, 6, 13). Although we acknowledge that cell behavior in culture may not directly reflect pacing in the intact heart, we did observe a range of activation voltages for I_h in a mixed population of zebrafish cardiac cells (data not shown), and it may be that primary pacemaking by I_h normally occurs only in those cells in which I_h activates at less negative voltages. It is also important to note that the difference between *smo* I_h and wild type I_h is dramatic throughout the entire range of I_h activation and is even larger with activation at less negative voltages (data not shown).

If I_h is important for pacemaking, why does nearly complete elimination of the fast component produce only a 2-fold change in the heart rate? Presumably there are several redundant or backup pacemaking mechanisms, as one might expect for a function so critical to survival. One of these might be the remaining slow component of I_h. Another could be the decay or a turnoff of outward K^+ current. In any case, it is interesting that disruption of a large component of I_h leaves rhythm and conduction sufficiently intact to permit development to proceed normally. This observation makes it reasonable to target subtypes of I_h for therapeutic purposes of slowing the heart, an important treatment for ischemic heart disease.

One candidate for the *smo* gene product is the channel protein that carries the I_h current or, more precisely, the fast component of I_h. However, it could also be another protein necessary for full I_h function. We have no evidence to distinguish the two, which ultimately rests upon the cloning and expression of the gene. I_h has not yet been cloned from any system or species. Therefore, because the molecular basis of pacemaking is so poorly understood, it will be important to achieve molecular definition of the *smo* gene, whether it is the channel or a regulator. A complete infrastructure for positional cloning is being assembled for the zebrafish. Framework maps have been generated, using microsatellites (30) and randomly amplified polymorphic DNA (31), and yeast artificial chromosome libraries are under construction (T. Zhong, E. Lander, and M.C.F., unpublished work). Clearly, *smo* will be a high priority as positional cloning in the zebrafish becomes more routine over the next few years.

We thank Margaret H. Boulos for her excellent technical assistance. This work was supported by: National Institutes of Health Grants R01 HL49579 (M.C.F.), R01 RR08888 (M.C.F.), T32 HL07208 (M.C.F.), and R01 NS29693 (G.Y.); a McKnight Investigator Award (G.Y.); a Research Starter Grant from the Foundation for Anesthesia Education and Research and the Society for Cardiovascular Anesthesiologists (K.B.); and a sponsored research agreement with Bristol Myers–Squibb (M.C.F.).

1. Hagiwara, N., Irisawa, H. & Kameyama, M. (1988) *J. Physiol. (London)* **395,** 233–253.
2. Noma, A., Morad, M. & Irisawa, H. (1983) *Pflugers Arch.* **397,** 190–194.
3. Campbell, D. L., Rasmusson, R. L. & Strauss, H. C. (1992) *Annu. Rev. Physiol.* **54,** 279–302.
4. Irisawa, H., Brown, H. F. & Giles, W. (1993) *Physiol. Rev.* **73,** 197–227.
5. DiFrancesco, D. (1991) *J. Physiol. (London)* **434,** 23–40.
6. DiFrancesco, D. (1993) *Annu. Rev. Physiol.* **55,** 455–472.
7. Brown, H. F., DiFrancesco, D. & Noble, S. J. (1979) *Nature (London)* **280,** 235–236.

8. Brown, H. & DiFrancesco, D. (1980) *J. Physiol. (London)* **308,** 331–351.
9. Yanagihara, K. & Irisawa, H. (1980) *Pflugers Arch.* **385,** 11–19.
10. DiFrancesco, D. (1981) *J. Physiol. (London)* **314,** 359–376.
11. DiFrancesco, D. (1981) *J. Physiol. (London)* **314,** 377–393.
12. Vassalle, M., Yu, H. & Cohen, I. S. (1995) *J. Gen. Physiol.* **106,** 559–578.
13. Yu, H., Chang, F. & Cohen, I. S. (1995) *J. Physiol. (London)* **485,** 469–483.
14. Yu, H., Chang, F. & Cohen, I. S. (1993) *Circ. Res.* **72,** 232–236.
15. Pape, H.-C. (1996) *Annu. Rev. Physiol.* **58,** 299–327.
16. Stainier, D. Y. R., Fouquet, B., Chen, J., Warren, K. S., Weinstein, B. M., Meiler, S., Mohideen, M. P. K., Neuhauss, S. C. F., Solnica-Krezel, L., Schier, A. F., Zwartkruis, F., Stemple, D. L., Malicki, J., Driever, W. & Fishman, M. C. (1996) *Development (Cambridge, U.K.)* **123,** 285–292.
17. Burggren, W. W. & Pinder, A. W. (1991) *Annu. Rev. Physiol.* **53,** 107–135.
18. Pelster, B. & Burggren, W. W. (1996) *Circ. Res.* **79,** 358–362.
19. Westerfield, M. (1995) *The Zebrafish Book: A Guide for the Laboratory Use of Zebrafish Danio rerio* (University of Oregon, Eugene, OR).
20. Kimmel, C. B., Ballard, W. W., Kimmel, S. R., Ullmann, B. & Schilling, T. F. (1995) *Dev. Dyn.* **203,** 253–310.
21. Hamill, O. P., Marty, A., Neher, E., Sakmann, B. & Sigworth, F. J. (1981) *Pflugers Arch.* **391,** 85–100.
22. Chen, J.-N., Haffter, P., Odenthal, J., Vogelsang, E., Brand, M., van Eeden, F. J. M., Furutani-Seiki, M., Granato, M., Hammerschmidt, M., Heisenberg, C.-P., Jiang, Y.-J., Kane, D. A., Kelsh, R. N., Mullins, M. C. & Nüsslein-Volhard, C. (1996) *Development (Cambridge, U.K.)* **123,** 293–302.
23. DiFrancesco, D. (1982) *J. Physiol. (London)* **329,** 485–507.
24. Denyer, J. C. & Brown, H. F. (1990) *J. Physiol. (London)* **429,** 401–409.
25. Iglewicz, B. (1983) in *Robust Scale Estimators and Confidence Intervals for Location*, eds. Hoaglin, D. C., Mosteller, F. & Tukey, J. W. (Wiley, New York), pp. 404–429.
26. DiFrancesco, D. & Tromba, C. (1987) *J. Physiol. (London)* **405,** 477–491.
27. DiFrancesco, D. & Tromba, C. (1988) *J. Physiol. (London)* **405,** 493–510.
28. DiFrancesco, D., Ducouret, P. & Robinson, R. B. (1989) *Science* **243,** 669–671.
29. Solomon, J. S., Doyle, J. F., Burkhalter, A. & Nerbonne, J. M. (1993) *J. Neurosci.* **13,** 5082–5091.
30. Knapik, E. W., Goodmann, A., Atkinson, S., Roberts, C. T., Shiozawa, M., *et al.* (1996) *Development (Cambridge, U.K.)* **123,** 451–460.
31. Postelthwait, J. H., Johnson, S. L., Midson, C. N., Talbot, W. S., Gates, M., Ballinger, E. W., Africa, D., Andrews, R., Carl, T., Eisen, J. S., Horne, S., Kimmel, C. B., Hutchinson, M., Johnson, M. & Rodriguez, A. (1994) *Science* **264,** 699–703.